Clustering of Binary Colloidal Suspensions: Experiment

MEHRDAD YASREBI, WAN Y. SHIH, AND ILHAN A. AKSAY

Department of Materials Science and Engineering and Advanced Materials Technology Center, Washington Technology Centers, University of Washington, Seattle, Washington 98195

Received April 25, 1989; accepted August 24, 1990

The stability of binary colloidal suspensions is examined and compared to that of particle–polymer systems. In particle–polymer systems, it is known that the addition of free polymers within a concentration range of polymers to a stabilized dispersion leads to flocculation. Similar to particle–polymer systems, we have observed that in binary colloidal suspensions, particles of the first kind can be induced to flocculate by the presence of particles of the second kind, within a certain range of concentration of the second kind of particles. Moreover, we have observed the growth of clusters of particles 1 at a later time in the initially restabilized regime. This slow growth of clusters in the initially restabilized suspensions is associated with the slowing of particle movement due to higher particle 2 concentrations. The aging phenomenon (growth of clusters) that occurs at high particle 2 concentrations clearly indicates that the seemingly restabilized suspension at high particle 2 concentrations is not due to thermodynamics, but to slow kinetics associated with slow particle movements at high densities. A similar aging phenomenon was observed with a particle–polymer (α-Al_2O_3/PAA) system in the seeming restabilization regime at high polymer concentrations.

I. INTRODUCTION

The phenomenon of flocculation of colloidal particles upon the addition of polymers to an initially dispersed colloidal suspension is now well established (1). The presence of free polymers can induce stable particles to undergo flocculation when the polymer concentration is above some value c^*. The flocculation rate of the colloidal particles peaks at some higher concentration $c^{***} > c^*$. When more free polymers are added, the flocculation rate decreases, and finally, at another concentration $c^{**} > c^{***}$, the suspension appears stabilized.

The process by which free polymers induce flocculation is referred to as *depletion flocculation* (2), and the one by which the restabilization of colloidal particles occurs at higher polymer concentrations is referred to as *depletion restabilization.* Depletion flocculation is attributed to an effective interparticle attraction due to the presence of free polymers (2, 3). As for depletion restabilization, two major theories exist which have quite different explanations. Feigin and Napper (2) suggested that an effective interparticle repulsive barrier develops at higher polymer concentrations. As the repulsive barrier grows with increasing polymer concentration, it will eventually slow the flocculation and give rise to restabilization. On the other hand, Fleer *et al.* (3) showed that the effective interparticle interaction is attractive at all polymer concentrations and restabilization is due to thermodynamics: i.e., the system becomes a one-phase system at high polymer concentrations. Despite the different explanations for the mechanism of the decrease in the flocculation rate in the restabilization regime, the two theories share a common ground. That is, both treat the polymers as a medium, which implicitly assumes that polymers always move fast enough to accommodate whatever change the movement of particles causes. This assumption may not be valid when the viscosity of the polymer solution is very high.

Recently, Liu *et al.* (4) have studied the stability of a binary-particle system using both

0021-9797/91 $3.00

Monte Carlo simulations and cluster variation method (CVM) calculations. They considered systems where only the interaction between particles of the first kind is attractive. They showed that the flocculation rate of particles 1 increases with particle 2 concentration and peaks at a certain particle 2 concentration. At higher particle 2 concentrations, the flocculation rate of particles 1 decreases with increasing particle 2 concentration. The phenomenon of the particle 1 flocculation rate peaking at a certain value of particle 2 concentration appears similar to the depletion flocculation and depletion restabilization phenomena occurring in particle–polymer systems. However, for the binary-particle systems, these authors showed that the decrease in the flocculation rate at higher particle 2 concentrations is due to slow particle movement at high concentrations, which is different from the thermodynamic (3) or the repulsive barrier (2) explanations proposed for the particle–polymer systems.

This paper presents our experimental studies on flocculation in both particle–particle and particle–polymer systems and compares the results of both systems. For particle–particle systems, conditions similar to those in the simulations in Ref. (4) were duplicated; i.e., the interaction between particles 1 is attractive, the interaction between particles 2 is repulsive, and that between particles 1 and particles 2 is repulsive. We found that, indeed, the initially stable suspensions of particles 1 were induced to flocculate by the presence of particles 2 when the particle 2 concentration was above some value c^*. The flocculation rate increased until it reached a maximum and then gradually decreased as the concentration of particles 2 was further increased. Finally, when the concentration of the second species was above some value c^{**}, the suspension became dispersed again.

To our knowledge, this is the first experimental observation of a stable–flocculation–restabilization type of transition occurring in a particle–particle system. Furthermore, we were able to observe the growth of clusters of particles 1, associated with the slowing of particle motion, in what seem to be restabilized suspensions at a later time. This aging phenomenon, the growth of clusters, that occurs at high particle 2 concentrations clearly indicates that the seeming restabilization at high particle 2 concentrations is a result of slow kinetics and not a result of thermodynamics. The slow kinetics at high particle 2 concentration is due to slow particle movement which is observable under the microscope. Thus, our observation agrees with the theoretical work of Liu *et al.* (4). In the particle–polymer systems we studied, i.e., alumina particles coated with polyacrylic acid (PAA) in PAA solutions, we also observed similar aging behavior in the seeming restabilization regime at high PAA concentrations where the viscosity of the suspensions is high. The growth of clusters in the initially restabilized regime at high PAA concentrations indicates that the seeming restabilization at high PAA concentrations is also due to slow particle movement.

The occurrence of similar transitions in both binary-particle systems and particle–polymer systems illustrates that the stable–flocculation–restabilization transition is not unique to particle–polymer systems. Furthermore, in both of the two binary-particle systems and the one particle–polymer system we studied the seeming diminishing of flocculation at high particle 2 or polymer concentrations is due to slow kinetics arising from slow particle movement. Thus, besides thermodynamics (3) and the repulsive interparticle interaction energy barrier (2), the observation of aging in our binary-particle systems and our particle–polymer systems suggests a third possibility for restabilization in a particle–polymer system, i.e., slow kinetics, at least for systems whose conditions are similar to ours. The slow kinetics we refer to here is the slow particle movement as evidenced in our experiments and in Ref. (4), which is different from the slow kinetics used in Ref. (2). In Ref. (2) particle motion was not addressed and the slow flocculation rate is due to the growth of the energy barrier with polymer concentration, which prohibits two particles from sticking to one another.

In this paper, the experimental systems are described briefly in Section II. The formulas we used to calculate the interparticle interaction are given in Section III. The results and the discussions are given in Section IV. Section V provides a summary.

II. EXPERIMENTAL

The colloidal particles used in this work consisted of α-Al_2O_3 particles of average diameter 0.64 μm (AKP-20, Sumitomo Chemical Company, Japan), SiO_2 particles of average diameter 0.74 μm prepared by the Stöber method (5), and acrylic-based latex of an average diameter of approximately 0.2 μm (Rhoplex AC552, Rohm & Haas Company). For both α-Al_2O_3/latex and α-Al_2O_3/PAA suspensions, polyacrylic acid of molecular weight (MW) 1800 was used as a stabilizing agent for α-Al_2O_3 particles (6) (PolySciences, Inc.). In the α-Al_2O_3/PAA suspensions, the free PAA molecules in the solution also have a molecular weight of 1800. For α-Al_2O_3/ SiO_2 suspensions, both α-Al_2O_3 and SiO_2 particles were not coated. The water was deionized and distilled, and the pH was adjusted with the addition of reagent-grade NaOH. The electrophoretic mobility of particles was measured with a zeta meter (Particle Micro-Electrophoresis, Rank Brothers, Cambridge, England).

To detect any flocculation in the system, each suspension was observed under an optical microscope (Leitz Metallovert Microscope, E. Leitz, Inc.). The general procedure is as follows. We first transferred a small drop of a suspension to a microscope coverglass, then placed another coverglass over it and sealed the edges immediately with a water-insoluble glue to prevent solvent evaporation. The suspension was examined under the microscope. An oil immersion lens was used to increase the resolution.

To further discern the makeup of the clusters, we examined slowly dried samples using scanning electron microscopy (SEM) with a Philips 515. The dried samples were prepared by placing a drop of the suspension on the SEM holder and allowing the drop to dry slowly.

III. INTERPARTICLE INTERACTIONS

We have estimated the interaction between particles of the ith species and particles of the jth species using the DLVO theory with the following form, in CGS units:

$$V(s_{ij}) = V_R(s_{ij}) + V_A(s_{ij}) \qquad [1]$$

where s_{ij} is the surface-to-surface distance along the center-to-center line between the particles. $V_A(s_{ij})$ is the attraction energy and can be approximated as (7)

$$V_A(S_{ij}) = \frac{-A_{i3j}}{12}\left[\frac{y}{x^2+xy+x} + \frac{y}{x^2+xy+x+y} + 2\ln\left(\frac{x^2+xy+x}{x^2+xy+x+y}\right)\right], \qquad [2]$$

where $x = S_{ij}/2R_j$, $y = R_i/R_j$, with R_i being the radius of the ith species particles and

$$A_{i3j} = (A_{ii}^{1/2} - A_{33}^{1/2})(A_{jj}^{1/2} - A_{33}^{1/2}), \qquad [3]$$

in which A_{ii} is the Hamaker constant of the ith species particles and A_{33} is that of water. In the following calculations, we use $A_{11} = 1.2 \times 10^{-12}$ erg for α-Al_2O_3, 0.86×10^{-12} erg for SiO_2, 0.66×10^{-12} erg for latex, and $A_{33} = 0.6 \times 10^{-12}$ erg for water. $V_R(s_{ij})$ is the repulsive interaction and can be approximated as

$$V_R(s_{ij}) = \frac{\epsilon\zeta_i\zeta_j R_i R_j}{s_{ij} + R_i + R_j}\, e^{-Ks_{ij}}, \qquad [4]$$

when $Ks_{ij} \ll 1$, where ζ_i is the ζ potential of the ith species particles, ϵ is the dielectric constant of water, K is the inverse screening length in the Debye–Hückel approximation,

$$K^2 = \frac{4\pi e^2}{\epsilon k_B T} \sum_i n_i z_i^2, \qquad [5]$$

where k_B is the Boltzmann constant, T the temperature, and n_i and z_i are the number density and charge of the ith species ions in the solution. In the following calculations, we use 1×10^{-2} M as the electrolyte concentration. The 10^{-2} M electrolyte concentration is estimated as follows. In the alumina/latex system, the estimated value is based on the induced couple plasma run on the supernatant of Rhoplex AC552, which revealed Na as the major electrolyte source with a concentration of 380 ppm, which is on the order of 10^{-12} M. In the case of alumina/silica systems, the alumina particles are uncoated, and the dissolution of alumina particles in basic solution forms ions of aluminum-containing complex with a concentration of about 10^{-3} to 10^{-2} M (8). We have also calculated the interparticle interactions at 10^{-3} M electrolyte concentration. All the interactions at 10^{-3} M electrolyte concentrations are essentially the same as those at 10^{-2} M except that the minimum in the alumina–alumina interaction is somewhat shallower.

IV. RESULTS AND DISCUSSION

For the α-Al_2O_3/latex systems, the experiments were carried out at pH 8 and at 2 vol% (volume percent) α-Al_2O_3 particles. The α-Al_2O_3 particles were stabilized using polyacrylic acid (PAA) of MW 1800. The adsorption of PAA on the α-Al_2O_3 surface has been well studied (6). At pH 8, PAA is negatively charged while the α-Al_2O_3 surface is overall positively charged. The opposite sign of the charge of PAA causes the adsorption of PAA onto the α-Al_2O_3 surface and consequently reverses the sign of the charge on the α-Al_2O_3 particles. At pH 8, the adsorption of PAA on the α-Al_2O_3 surface is so strong that it barely desorbs (6). In our experiment with the α-Al_2O_3/latex suspensions, we chose the PAA concentration at the onset of the plateau of the adsorption isotherm. Therefore, the α-Al_2O_3 particles are covered with the saturated amount of PAA, while there is no excess PAA in the suspensions. Under such conditions, the PAA-covered α-Al_2O_3 particles have a ζ potential of −40 mV. The latex particles have a ζ potential of −60 mV. As we have mentioned above, the adsorption of PAA on the α-Al_2O_3 surface is very strong and one can regard a PAA-covered α-Al_2O_3 particle as a unity. This point is further supported by the result of the infrared (IR) reflectance studies which showed that the mixing of the PAA-covered α-Al_2O_3 particles with the latex particles *did not* result in any shift in the IR spectrum of the PAA-covered α-Al_2O_3 particles or in that of the latex particles. Therefore, the transfer of the surface additives from one species of particles to another (i.e., PAA from α-Al_2O_3 to latex and the surfactant from latex to α-Al_2O_3) is minimal in our experiments. Below, we will simply refer to the PAA-covered α-Al_2O_3 particles as "α-Al_2O_3 particles" for convenience.

Samples were prepared by adding latex particles of various concentrations to suspensions of 2 vol% α-Al_2O_3. The excess H_2O was then evaporated to keep α-Al_2O_3 particles at 2 vol%. Each suspension was ultrasonicated to ensure uniform mixing prior to examination under the microscope.

The calculated interparticle interaction energies in the α-Al_2O_3/latex suspensions are shown in Fig. 1, where the interaction energies are in units of k_BT, where T is the room temperature. One can see that the interactions between latex particles and between the latex particles and the α-Al_2O_3 particles are basically repulsive since in both curves the second minimum is very shallow compared to k_BT, and that the barrier before the primary minimum is very high. The interaction between α-Al_2O_3 particles also has a high barrier before the primary minimum, so that a primary-minimum type of flocculation between α-Al_2O_3 particles is practically prevented. However, the depth of the second minimum is about 1 k_BT. Hence, under the experimental condition, the α-Al_2O_3 particles are weakly attractive and may be induced to flocculate by some repulsive species such as the latex particles since the energetic conditions of the α-Al_2O_3/latex suspension are very similar to those of the simulations from Ref. (4).

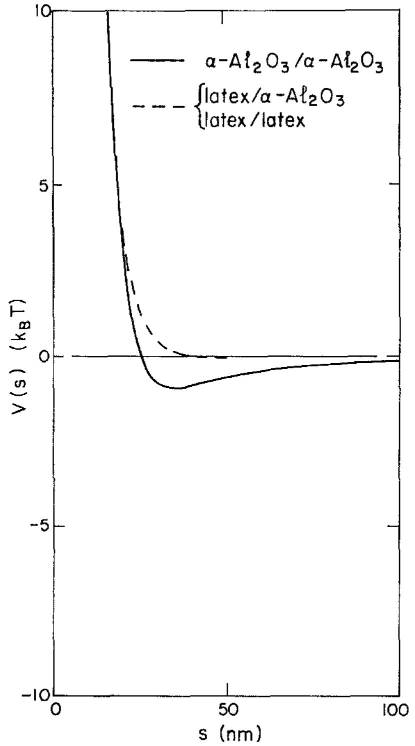

FIG. 1. $V(s)$ vs s for the α-Al_2O_3/latex system at pH 8 where $V(s)$ is the interparticle interaction energy in units of k_BT and s is the interparticle surface-to-surface distance along the center-to-center line. The ζ potential for the α-Al_2O_3 particles is −40 mV and that for the latex particles is −60 mV. The radius of the latex particles is 0.1 μm and that of the α-Al_2O_3 is 0.32 μm. The electrolyte concentration is taken to be 1.0×10^{-2} M. Note that the α-Al_2O_3 particles in this case are coated with PAA.

As an example of the stable–flocculation–restabilization transition in a particle–particle system, we have plotted in Fig. 2 the floc size of the α-Al_2O_3/latex suspensions after 15 min of aging versus the concentration of latex particles. The concentration of the α-Al_2O_3 particles is kept at 2 vol%. When the latex particles were added to the initially dispersed α-Al_2O_3 suspensions, the stability of the α-Al_2O_3 particles was unaffected up to about 15 vol% of latex particles. The α-Al_2O_3 particles started to flocculate as the concentration of latex particles rose above 15 vol%. The cluster size increased until it reached a maximum at about 30 vol% of latex particles and then gradually decreased as the concentration of the latex particles was further increased. Finally, when the latex concentration was above about 58 vol%, the α-Al_2O_3 particles became dispersed again. Examples of microstructures of the suspensions in the stable, flocculated, and restabilized regimes are shown in Figs. 3a–c. The latex particles do not show in the micrographs due to their small size and rapid Brownian motion. However, in the experiments, one can actually see the latex particles under the optical microscope. In all the experiments, the latex particles remained stable, i.e., well separated and uniformly distributed throughout the suspension, indicative of the repulsive interaction between the latex particles as a result of the high ζ potential, as we have shown in Fig. 1. Figures 3a and c show the microstructures in the stable and the restabilized regimes, respectively. In these regimes α-Al_2O_3 particles were well separated and uniformly distributed throughout the suspension, with each particle exhibiting Brownian motion. Figure 3b shows a typical microstructure of a suspension in the flocculated regime where clusters of α-Al_2O_3 particles were visible. Within the clusters, particles are frozen. Furthermore, the cluster size varied with the latex concentration in the flocculated regime, as shown in Fig. 2; therefore,

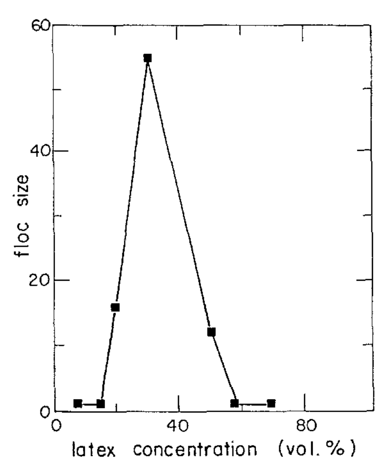

FIG. 2. Cluster size as a function of concentration of latex particles (α-Al_2O_3 particles are kept at 2 vol%). The units of the clusters are arbitrary. All the data points are taken after 15 min of suspension aging.

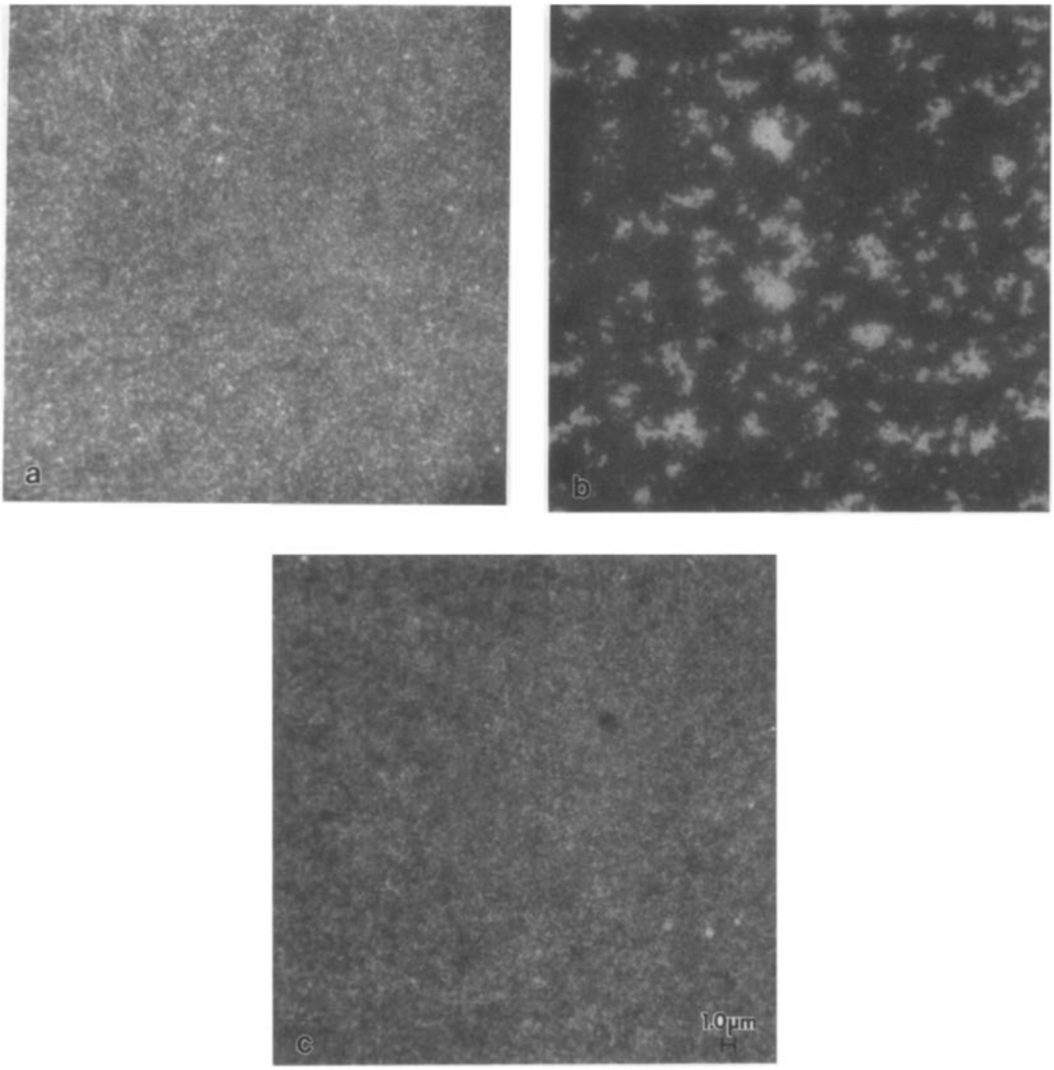

FIG. 3. Microstructures of suspensions in (a), (b), and (c) correspond to micrographs of suspensions in the stable, flocculated, and restabilized regimes. The scale shown in (c) also applies to the other micrographs in this figure.

the microstructures looked different at different latex concentrations. On the contrary, no discernible microstructural difference was observed as a function of the latex concentration in the stable and the restabilized regimes.

Although the "short-time" microstructures look the same in the stable and the restabilized regimes, we found that the kinetic behavior in the restabilized regime at high latex concentrations was very different from that in the stable regime at low latex concentrations. In the stable regime, particles move vigorously, and we did not observe any change in the suspensions with time, whereas, in the flocculated and, especially, in the restabilized regimes, particles become less mobile or motionless and the microstructures of the suspensions change with time. Moreover, the growth of clusters of α-Al_2O_3 particles was slower for suspensions of higher latex concentrations. For example, it took longer for the restabilized suspension with 70 vol% of latex particles to form clusters than the suspension with 58 vol% of latex particles. The slow flocculation rate at high particle 2 concentrations is consistent with the observed slowing of particle movement.

The observation of the aging effect in the flocculated and the restabilized regimes indicates that the restabilization of α-Al_2O_3 particles is due to slow kinetics, not to thermodynamics. The slowing of the flocculation rate of α-Al_2O_3 particles at higher latex concentrations is due to the hindrance of particle movement. To further clarify this point, we have also done experiments on the α-Al_2O_3/SiO_2 suspensions under similar conditions, i.e., the interaction between α-Al_2O_3 particles is attractive and the rest of the interactions (SiO_2/SiO_2, α-Al_2O_3/SiO_2) are repulsive. The details of the experiments are as follows: 2 vol% α-Al_2O_3 suspensions were mixed with different concentrations of SiO_2 particles. The preparation method was similar to the experiment illustrated in Fig. 1, except that in the α-Al_2O_3/SiO_2 experiment, the suspensions were prepared electrostatically at pH 9; that is, PAA was *not* used in this system. At pH 9, SiO_2 particles are highly repulsive, i.e., with a ζ potential of nearly -110 mV and very stable. On the other hand, α-Al_2O_3 particles have a low ζ potential of -10 mV at pH 9 and are highly flocculated even at 2 vol% concentration.

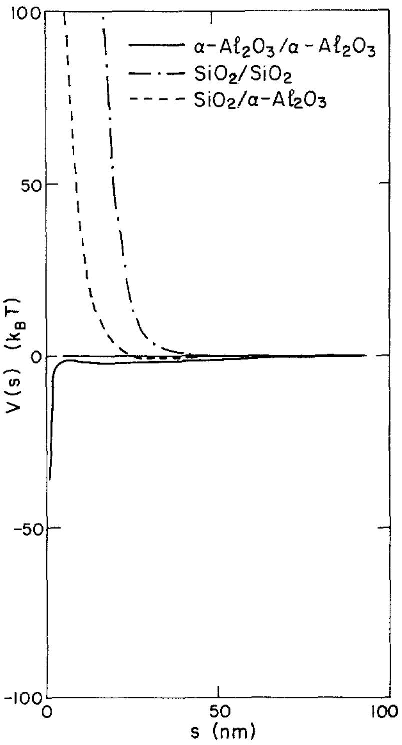

FIG. 4. $V(s)$ vs s for the α-Al_2O_3/SiO_2 system at pH 9 where $V(s)$ and s are the same as in Fig. 1. The ζ potential of the α-Al_2O_3 particles is -10 mV and that of the SiO_2 particles is -110 mV. The radius of the α-Al_2O_3 particles is 0.32 μm and that of the SiO_2 particles is 0.37 μm. The electrolyte concentration is taken to be 1.0×10^{-2} *M*. Note that the α-Al_2O_3 particles in this case are *not* coated with PAA.

The calculated interparticle interactions of the α-Al_2O_3/SiO_2 system are shown in Fig. 4. One can see that, again, the interaction between the SiO_2 particles and the α-Al_2O_3 particles is practically repulsive. The interaction between the α-Al_2O_3 particles is extremely attractive due to the vanishing of the repulsive barrier before the primary minimum, so that the α-Al_2O_3 particles can be highly flocculated even at a very low concentration. With the α-Al_2O_3/SiO_2 system, we were able to study the restabilization regime (the right-hand half of Fig. 2) more closely. Figure 5 shows the cluster size in the α-Al_2O_3/SiO_2 suspensions as a function of SiO_2 concentration after 15 min of aging. Without SiO_2 particles, the 2 vol% α-Al_2O_3 suspension was highly flocculated, as mentioned, and the cluster size decreased as the SiO_2 particles were added to the suspension. The aging effect in the restabilized regime is shown in the insert in Fig. 5, where the cluster size at 48 vol% SiO_2 is shown to increase with time.

To illustrate that the clustering occurs mainly among the α-Al_2O_3 particles, examples of SEM micrographs are shown in Figs. 6a and b. Figure 6b is a blowup of part of Fig. 6a. The sample was dried from a drop of a suspension consisting of 2 vol% α-Al_2O_3 and 5 vol% SiO_2. One can see that (i) SiO_2 particles (spheres) and α-Al_2O_3 particles (irregularly shaped) do not mix and (ii) clustering occurs

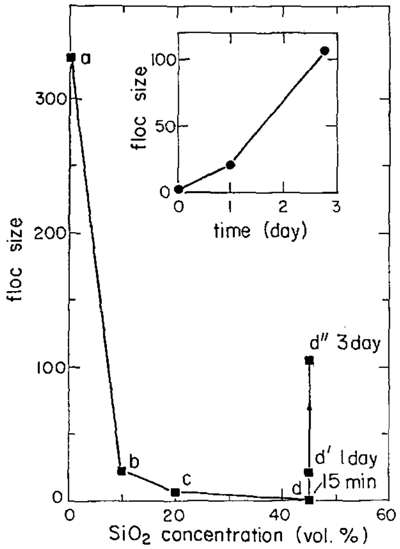

FIG. 5. Cluster size of α-Al_2O_3 particles at pH 9 as a function of SiO_2 concentration after 15 min of suspension aging (points a–d) and at different times (points d–d″). The insert shows the cluster size as a function of time at 48 vol% SiO_2 (points d–d″). α-Al_2O_3 particles are kept at 2 vol%. The units of the clusters are arbitrary.

mainly among the α-Al_2O_3 particles, as evidenced in both Figs. 6a and b.

The microstructures of the suspensions at various SiO_2 concentrations and at different times are shown in Figs. 7a–d″. Figure 7a illustrates the state of flocculation of a 2 vol% α-Al_2O_3 suspension at pH 9, where large clusters form almost instantly. In Figs. 7b and c, where the suspensions have 10 and 20 vol% SiO_2 particles, respectively, the cluster size decreased. In Fig. 7d at 48 vol% SiO_2, the α-Al_2O_3 clusters almost disappeared. Figures 7d′ and d″ show the microstructures of α-Al_2O_3 clusters at 48 vol% SiO_2 particles after 1 and 3 days of aging, respectively. As in the α-Al_2O_3/latex system, the particle movements become slower in the restabilized regime at high SiO_2 concentrations. It is clearly seen that clusters of α-Al_2O_3 particles grow from the

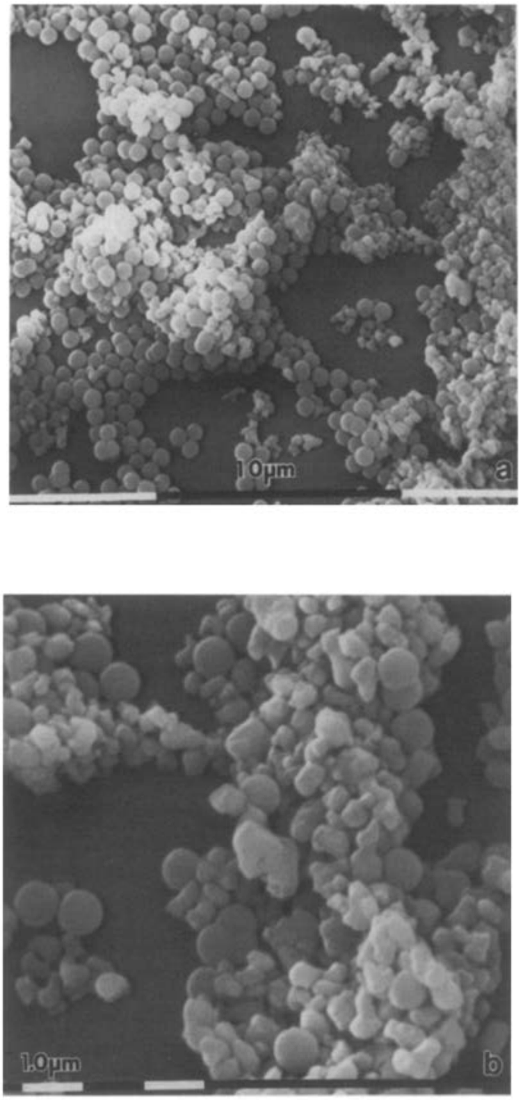

FIG. 6. SEM micrographs of a dried sample from a suspension of 2 vol% α-Al_2O_3 and 5 vol% SiO_2. The SEM sample was prepared by placing one drop of the suspension on the SEM sample holder and allowing the drop to dry slowly. (a) Low-magnification micrograph, (b) blowup of part of (a). Note that clustering occurred mainly among α-Al_2O_3 particles (irregularly shaped) and that the SiO_2 particles and the α-Al_2O_3 particles do not mix. The average radius of the SiO_2 particles in 0.37 μm and that of the α-Al_2O_3 particles is 0.32 μm.

FIG. 7. Microstructures of the suspensions in Fig. 5. (a) 0 vol% SiO_2, (b) 10 vol% SiO_2, (c) 20 vol% SiO_2, (d) 48 vol% SiO_2, (d′) suspension in (d) after 1 day of aging, (d″) suspension in (d) after 3 days of aging. The scale shown in (d″) also applies to other micrographs in this figure.

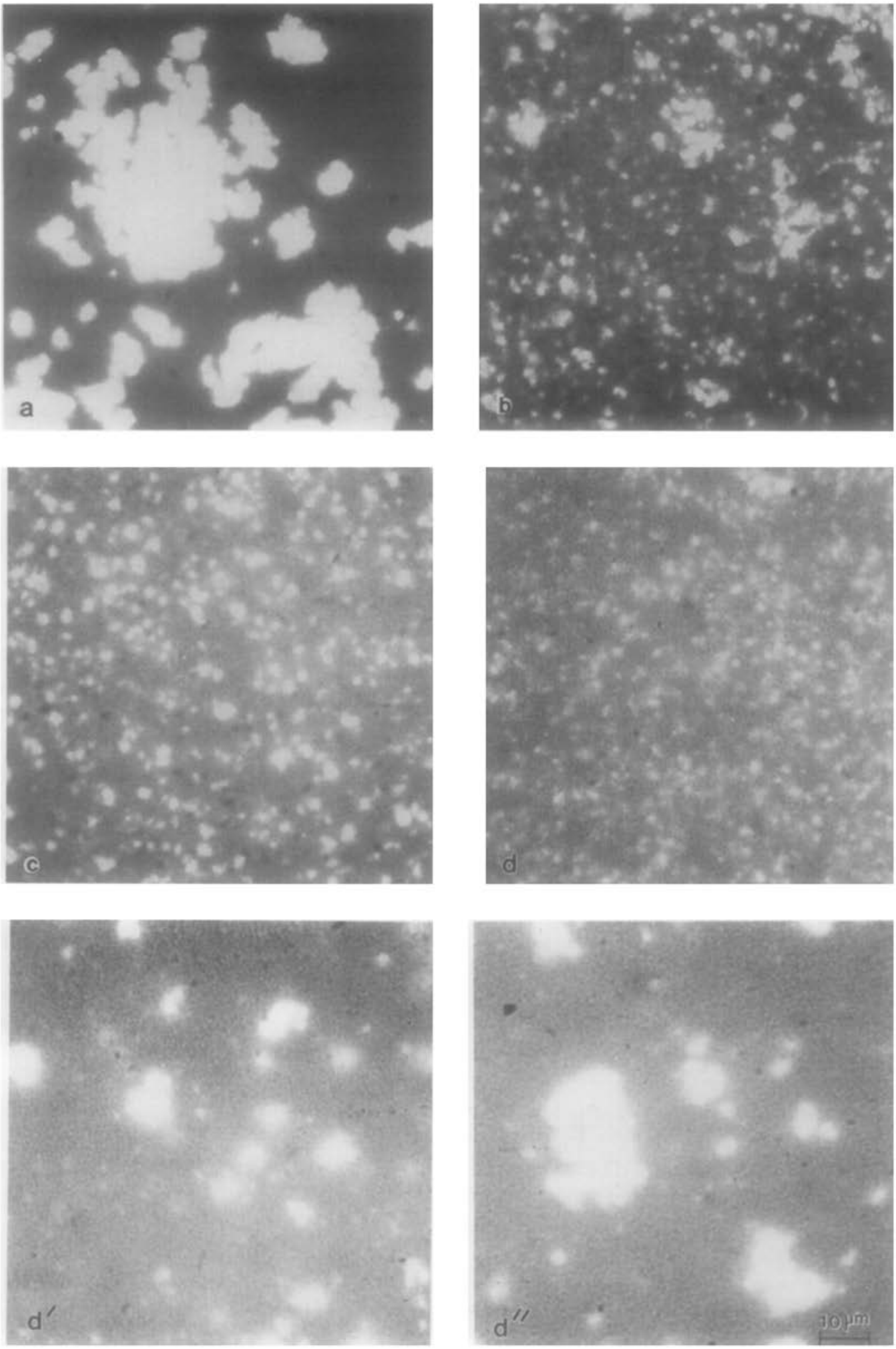
a
b
c
d
d′
d″
10 μm

initially restabilized suspensions. It is worth noting that in all SiO_2 concentrations, SiO_2 particles are visible in the micrograph as well-separated and uniformly distributed particles in the background, again indicating the repulsive interaction between SiO_2 particles throughout all SiO_2 concentrations.

The aging phenomenon observed in the seemingly restabilized region in a binary-particle system such as the α-Al_2O_3/latex system or the α-Al_2O_3/SiO_2 system was also observed in a particle–polymer system, specifically PAA-coated α-Al_2O_3 particles with free PAA. In the following, we will again refer to the PAA-coated α-Al_2O_3 particles simply as α-Al_2O_3 particles for convenience. The α-Al_2O_3 particles are kept at 2 vol% and the pH at 8. Here the PAA-covered α-Al_2O_3 particles are negatively charged and have a ζ potential of -40 mV. The PAA is also negatively charged. Figure 8 shows the cluster size of the α-Al_2O_3 particles after 2 min of aging as a function of the free PAA concentration. The peak in the cluster size as a function of PAA concentration, c, is as expected for a particle–polymer system. However, Fig. 8 also shows the aging effect in the high PAA concentration region where initially the cluster size is small. The clusters grow at a later time in the seemingly restabilized regime, similar to the observation of a binary-particle system. The insert in Fig. 8 shows the cluster size at $c = 21.6$ wt% as a function of time. The microstructures of the α-Al_2O_3/PAA system at various points of Fig. 8 are shown in Figs. 9a–c″ where Fig. 9a corresponds to point a in Fig. 8, Fig. 9b to point b in Fig. 8, and so on. The slow flocculation rate in the seeming restabilization regime is also due to slow particle movement at high PAA concentrations. Even though the PAA is charged in our experiment, the charge may change the onset concentration but should not make much difference in the overall behavior at high concentrations. The aging we observed with PAA at high concentrations should also occur in a neutral polymer solution. The reason is as follows. In dilute solutions, the conformation of a PAA chain is more extended due to the long-ranged Coulomb repulsion between monomers and is therefore different from that of a neutral polymer of the same molecular weight. However, at high concentrations such as those in our experiment, the long-range Coulomb repulsion between monomers is screened by the counterions released by the monomers and also by the presence of other monomers. The intermonomer interaction is therefore short-ranged as in a neutral polymer solution and the conformation of a polyelectrolyte chain is no longer extended but rather more like that of a neutral polymer at high concentrations (9).

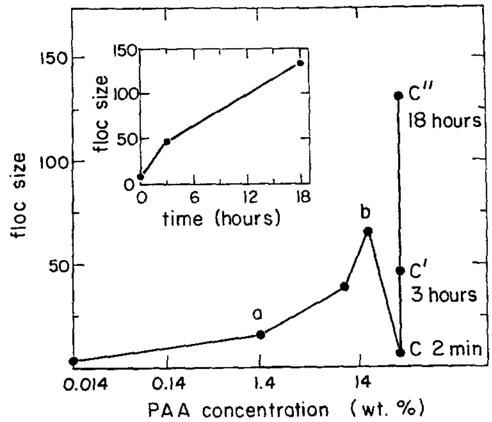

FIG. 8. Cluster size vs free PAA concentration. Al_2O_3 particles are kept at 2 vol%. The cluster size was measured after 2 min of aging. The insert shows the cluster size as a function of time at $c = 21.6$ wt% (points $c - c''$).

V. SUMMARY

In summary, we have shown experimentally that in binary colloidal suspensions, as the

FIG. 9. Microstructures of suspensions at different free PAA concentrations. (a) corresponds to point a in Fig. 8 and (b) to point b in Fig. 8, and so on. The scale shown in (c″) also applies to other micrographs in this figure.

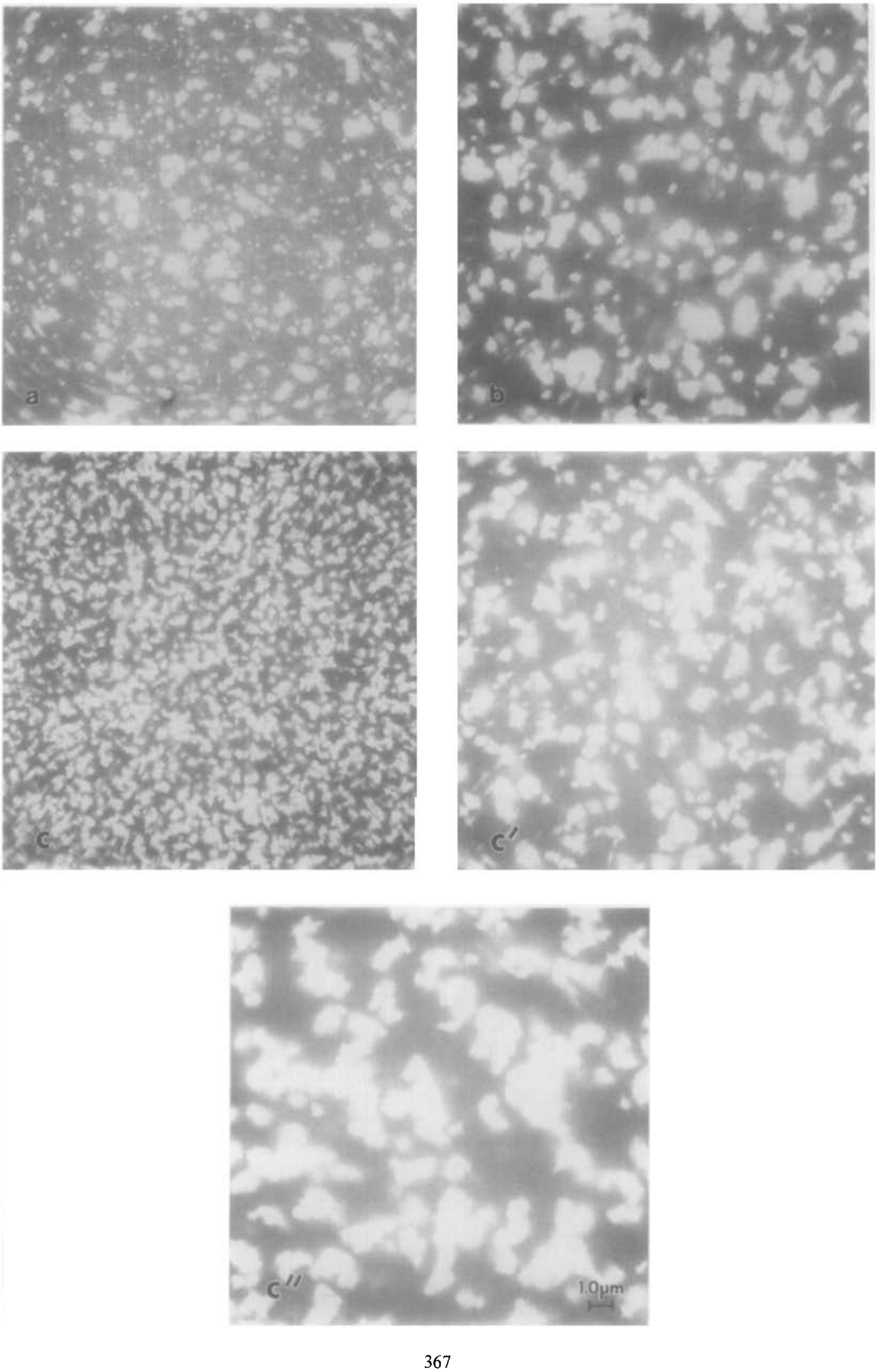
a
b
c
c′
c″
1.0μm

colloidal particles of the second kind, e.g., latex or SiO_2, with repulsive (or less attractive) interactions were added to suspensions of particles of the first kind, e.g., α-Al_2O_3, with weakly attractive interactions, the first kind of particles go through a stable–flocculation–restabilization transition as the concentration of particles of the second kind is increased, similar to what is observed in particle–polymer systems when the polymer concentration is increased. The underlying mechanism for the seeming restabilization at high particle 2, i.e., latex or SiO_2, concentrations is attributed to slow kinetics at high densities and not to thermodynamics. Here, by slow kinetics we mean slow particle movements, which are observable under an optical microscope. Our observation is in agreement with the simulation of Ref. (4) where with similar energetic conditions, i.e., $E_{11} < 0$, E_{12}, and $E_{22} > 0$, it was shown that slow particle movements give rise to the seeming restabilization at high particle concentrations. Thus, the peak in the flocculation rate (Fig. 2) is only the manifestation of slow kinetics at higher particle concentrations. In the work reported in Ref. (4), the free energy of the binary-particle systems was also calculated and showed that the underlying equilibrium state for flocculation (including the seemingly restabilized states) is phase separation. Therefore, the flocculated state is really a result of a kinetic effect and the nonequilibrium manifestation of phase separation.

Furthermore, for the particle–polymer system we studied, the α-Al_2O_3/PAA system, similar aging phenomena occur in the seeming restabilization region at high PAA concentrations and the aging is also associated with slow particle movement. Although the work cited in Ref. (2) also suggested that the restabilization at high polymer concentrations is due to kinetics for polymer–particle systems, the slow flocculation kinetics is due to the growth of the repulsive barrier in the effective interparticle interaction with polymer concentration rather than the slowdown of the particle movements as we have observed in the present systems. Thus, our observation of aging in both the binary-particle system and the α-Al_2O_3/PAA system illustrates that slow particle movements at high densities are also a possible cause for the depletion stabilization of a particle–polymer system, at least for systems whose conditions are similar to ours.

ACKNOWLEDGMENTS

This work was supported by the Air Force Office of Scientific Research (AFOSR) and the Defense Advanced Research Projects Agency (DARPA) under Grant AFOSR-87-0114.

REFERENCES

1. For a review, see Napper, D. H., *in* "Polymeric Stabilization of Colloidal Dispersions," Chaps. 15–17. Academic Press, London/New York, 1985.
2. Feigin, R. I., and Napper, D. H., *J. Colloid Interface Sci.* **75**, 525, (1980); also see Ref. (1).
3. Fleer, G. J., Scheutjens, J. H. M. H., and Vincent, B., *ACS Symp. Ser.* **240**, 245 (1984).
4. Liu, J., Shih, W. Y., Kikuchi, R., and Aksay, I. A., *J. Colloid Interface Sci.* **142**, 369 (1991).
5. Stöber, W., Fink, A., and Bohn, E., *J. Colloid Interface Sci.* **26**, 62 (1968).
6. Yasrebi, M., Ph.D. thesis, University of Washington, Seattle, 1988, Chap. 5.
7. Shaw, D. J., "Introduction to Colloidal and Surface Chemistry," 3rd ed., pp. 188–89. Butterworths, London, 1980.
8. Nakagawa, H., Yasrebi, M., Liu, J., and Aksay, I. A., unpublished.
9. Aguilera-Granja, F., and Kikuchi, R., unpublished.